LAWRENCE
LIVERMORE
NATIONAL
LABORATORY

UCRL-PROC-220549

Mitigation of Laser Damage Growth in Fused Silica NIF Optics with a Galvanometer Scanned Carbon Dioxide Laser

Isaac L. Bass, Vaughn Draggoo, Gabriel M. Guss, Richard P. Hackel, Mary A. Norton

April 11, 2006

2006 SPIE "High-Power Laser Ablation"
Taos, NM, United States
May 7, 2006 through May 12, 2006

Mitigation of Laser Damage Growth in Fused Silica NIF Optics with a Galvanometer Scanned CO_2 Laser

Isaac L. Bass*, Vaughn G. Draggoo, Gabriel M. Guss, Richard P. Hackel, Mary A. Norton

University of California
Lawrence Livermore National Laboratory
P.O. Box 808, L-592
Livermore, CA 94550

ABSTRACT

Economic operation of the National Ignition Facility at the Lawrence Livermore National Laboratory depends on controlling growth of laser damage in the large, high cost optics exposed to UV light at 351 nm. Mitigation of the growth of damage sites on fused silica surfaces greater than several hundred microns in diameter has been previously reported by us using galvanometer scanning of a tightly focused 10.6 µm CO_2 laser spot over an area encompassing the laser damage. Further investigation revealed that fused silica vapor re-deposited on the surface as "debris" led to laser damage at unexpectedly low fluences when exposed to multiple laser shots at 351 nm. Additionally, laser power and spatial mode fluctuations in the mitigation laser led to poor repeatability of the process. We also found that the shape of the mitigation pit could produce downstream intensification that could damage other NIF optics. Modifications were made to both the laser system and the mitigation process in order to address these issues. Debris was completely eliminated by these changes, but repeatability and downstream intensification issues still persist.

Keywords: Mitigation, CO_2, fused silica, laser damage, galvanometer, scanning

1. INTRODUCTION

The National Ignition Facility shown in Fig. 1 (NIF) at the Lawrence Livermore National Laboratory (LLNL) is designed to ignite the sustained fusion of a deuterium-tritium target with 1.8 MJ of 351 nm, UV laser light. This UV light is produced by tripling a highly-amplified (~10^{15} amplification) 1053 nm beam just before the final optics that focus the beam onto the target (Fig. 1). Surface damage to the final fused silica optics by the UV light limits the maximum fluence at which the NIF can operate. Initiation of damage on these optics is expected at the fluences planned for NIF operation, and this damage will grow with additional NIF laser shots. Economic operation of the NIF will depend on mitigating (preventing) damage growth on the large, high-cost, final optics that operate at 351 nm.

An in-situ diagnostic in the NIF identifies damage created during NIF operation and monitors its growth. It is allowed to grow to the maximum size that still permits successful mitigation with our current techniques (between 300 and 500 µm in its lateral dimensions). At this point the optic is removed from service. The damage is mitigated in an off-line facility by removing the damaged material and restoring a small area around it to a form that will not damage when the optic is returned to NIF operation.

Damage is locally removed by a combination of evaporation and melting produced by a tightly focused, 10.6 µm, CO_2 laser beam that is very strongly absorbed at the surface. Successful mitigation of damage sites less than ~100 µm in their transverse dimensions (i.e., average diameter) has been demonstrated using one or several pulses of the CO_2 laser.[1,2] For larger damage sites, a more complex technique was developed that involved galvanometer scanning of the laser spot[3] (Fig. 1). This technique also involved a step where the fused silica re-deposited on the surface as debris

* Correspondence: Email: bass1@llnl.gov, Mailstop: L-592, Telephone: 925-423-8389, Fax: 925-422-5099

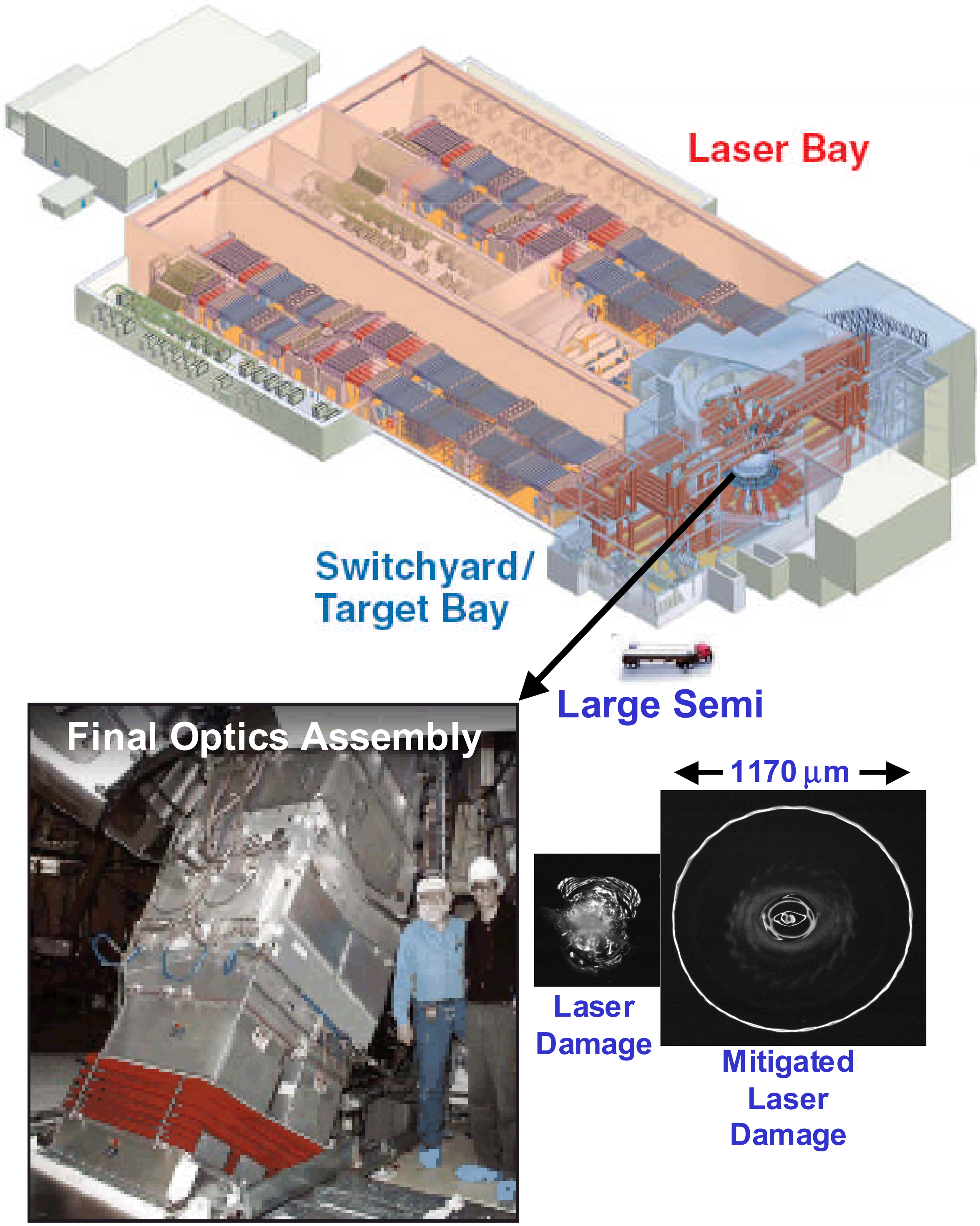

Fig. 1 (Top) Sectional view of the NIF facility showing the laser bay and the target bay that houses the target chamber. (Lower left) A final optics assembly for 4 of the 192, ~40 x 40 cm^2, NIF beams that is mounted on the side of the 10 m diameter target chamber. The assembly contains the crystals that convert the 1053 nm light to 351 nm light, and the fused silica lens that focuses the 351 nm light onto the target. (Lower right) Example of laser damage on fused silica produced by the 351 nm light, and the appearance after it has been mitigated using galvanometer scanning of a tightly focused, 10.6 µm CO_2 laser beam.

during evaporation was re-melted by scanning the CO_2 beam at a lower power. We refer to this step as "passivation" because it reduces the tendency of this debris to damage when exposed to the UV beam at NIF fluences.

The susceptibility of laser damage mitigated by this scanning technique to further damage was first tested by raster scanning the focused 355 nm laser spot from a commercial, pulsed Nd:YAG laser over the mitigated damage site. The ~800-µm, $1/e^2$-diameter of the 355 nm spot was smaller than the ~1 mm diameter of the mitigated damage site. The beam was scanned over the mitigation site 4 times to account for pulse-to-pulse pointing fluctuations caused by air turbulence. In these tests, the mitigated sites survived to fluences >22 J/cm^2 at 7.5 ns pulse length (equivalent to the highest 351 nm fluences expected in NIF operation with regard to re-initiation of laser damage).

However, when tests were performed with a 5 mm-diameter, approximately top-hat, 351-nm beam from a Nd:YLF/ Glass laser, damage to the mitigated sites would sometimes occur at fluences as low as 6 J/cm^2 for a 10 ns pulse. It was observed that the damage initiated at locations inside the mitigated site where debris was incompletely passivated. To address this problem, we introduced a final passivation step with a larger CO_2 spot, scanned at slower speeds, and at a power level that maintained the temperature just below the evaporation threshold. This step was intended to produce a more complete passivation by melting the debris into a form close to the original fused silica without generating new debris. It was also hoped that this step would smooth features in the mitigation site believed to cause downstream intensification of the NIF beam.

Modifications were also made to the operating mode of the CO_2 laser and the optical delivery system that were intended to correct the effects of periodic fluctuations in the laser output power and spatial mode on process repeatability.

We report on the impact that these changes had on the damage resistance and downstream intensification of the mitigated damage sites, and on the process repeatability.

2. THE NEW PASSIVATION PROCESS AND LASER OPERATION

The $1/e^2$-diameter of the CO_2 beam in the original scanning mitigation technique[3] was ~200 µm for both evaporation and passivation. Evaporation involved an inward moving spiral in which the power was varied between roughly 2 W and 15 W to achieve the desired shape of the pit. The CO_2 laser was operated pulsed at 5 kHz, and its power was varied by changing the pulse length (i.e., the duty factor). Passivation involved an outward moving spiral with power being varied between roughly 0.5 W and 6 W. The evaporation/passivation sequence would be repeated multiple times as necessary depending on the diameter and depth of the damage site being mitigated.

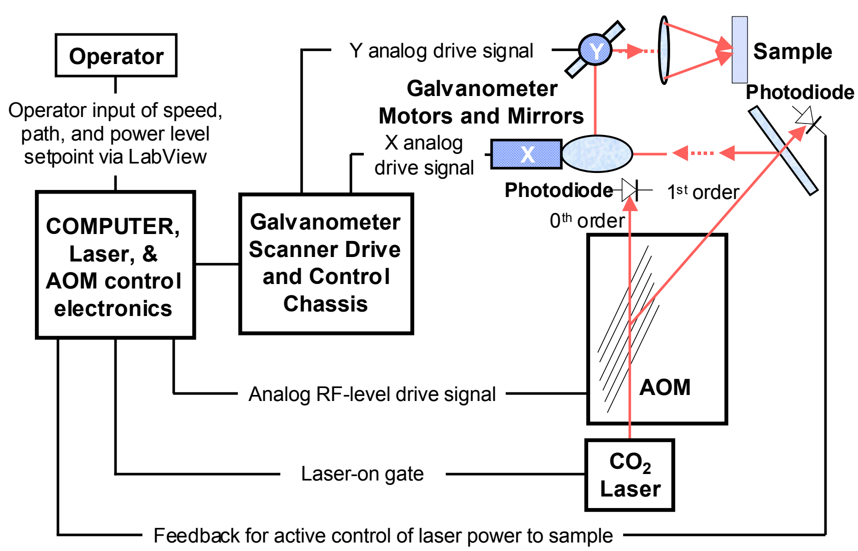

Fig. 2 Schematic diagram of the CO_2 optical delivery system showing active power control with the acousto-optic modulator.

The CO_2 spot was increased for the new, large-beam passivation. The focusing lens was moved away from the sample until the $1/e^2$-diameter of the spot was roughly 500 µm. The passivation involved three separate steps that spiraled the spot first along the perimeter, then around the walls, and finally around the center of the mitigation site. The power was adjusted throughout these spirals to maintain the surface temperature just below the evaporation threshold.

To improve process repeatability, the operation of the CO_2 laser was switched from pulsed to CW, and an acousto-optic modulator (AOM) was inserted in the beam path to permit active control of power delivered to the sample (see Fig. 2).

Insertion of the AOM reduced the maximum power available at the sample from 15 W to ~8 W. This required reduction of the scan rate and an increase of the duration of the spiral for both the evaporation and small-beam passivation spirals. The new inward moving evaporation spiral starts from a radius between 360 and 470 µm (depending on the number of repetitions) and ends at a radius of 10 µm. The spiral pattern is expanded by 3% between repetitions from 1 to 9 repetitions, and then the identical 9-repetition expansion sequence is repeated multiple times as needed. Each evaporation spiral has 62.25 cycles and a duration ranging between 550 and 685 ms for 1 to 9 expansion repetitions. The average spot speed is 175 mm/s with a maximum of 200 mm/s. The final radius of the outward moving small-beam passivation spiral varies between 400 and 520 µm for 1 to 9 expansion repetitions. Its duration varies correspondingly between 355 and 415 ms.

3. EFFECTS OF LARGE-BEAM PASSIVATION STEP ON RE-DEPOSITED DEBRIS

Figure 3 shows microscope images and contour interferograms of a representative mitigation site before and after the final large-beam passivation step. After this step, light scattered from debris inside the mitigation site is no longer visible indicating that the debris has been converted into a specularly smooth fused silica surface that scatters less light.

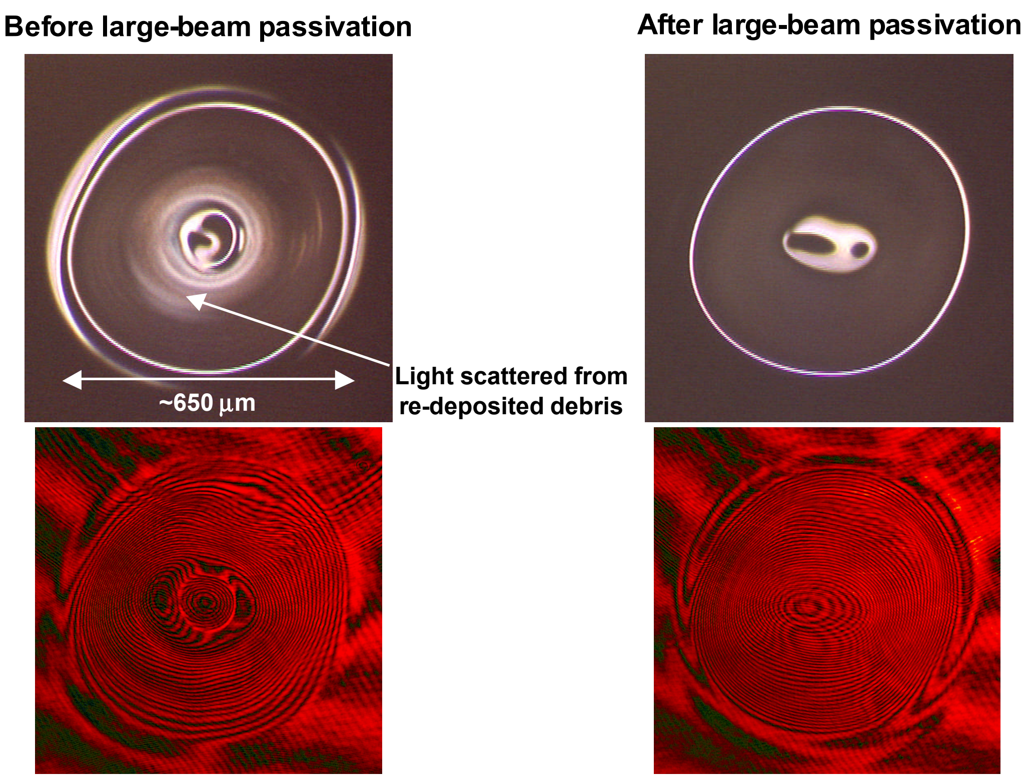

Fig. 3 Microscope images of a mitigation site show that light scattering from debris has been virtually eliminated by the large-beam passivation. Larger scale smoothing effects in the bottom and around the perimeter are also evident in both the microscope images and the contour intereferograms.

Larger scale surface features in the bottom and around the perimeter of the site have apparently also been smoothed as is evident in both the microscope images and the interferograms.

Scanning electron microscope (SEM) images shown in Fig. 4 confirm that the debris has been converted into a form essentially equivalent to that of a smooth fused silica surface. High magnification (20,000X) images were taken on the walls of the mitigation crater where the debris is normally heaviest. A fibrous structure of the debris is clearly evident prior to the large-beam passivation (the details of this structure vary depending on the number of evaporation/passivation repetitions performed prior to large beam passivation). The high magnification images on the walls after the large beam passivation reveal no surface structure above the noise floor of the instrument (~10 nm). Carbon particles were intentionally placed on the surface to facilitate focusing because there were no distinguishable features in the fused silica itself at the high magnifications.

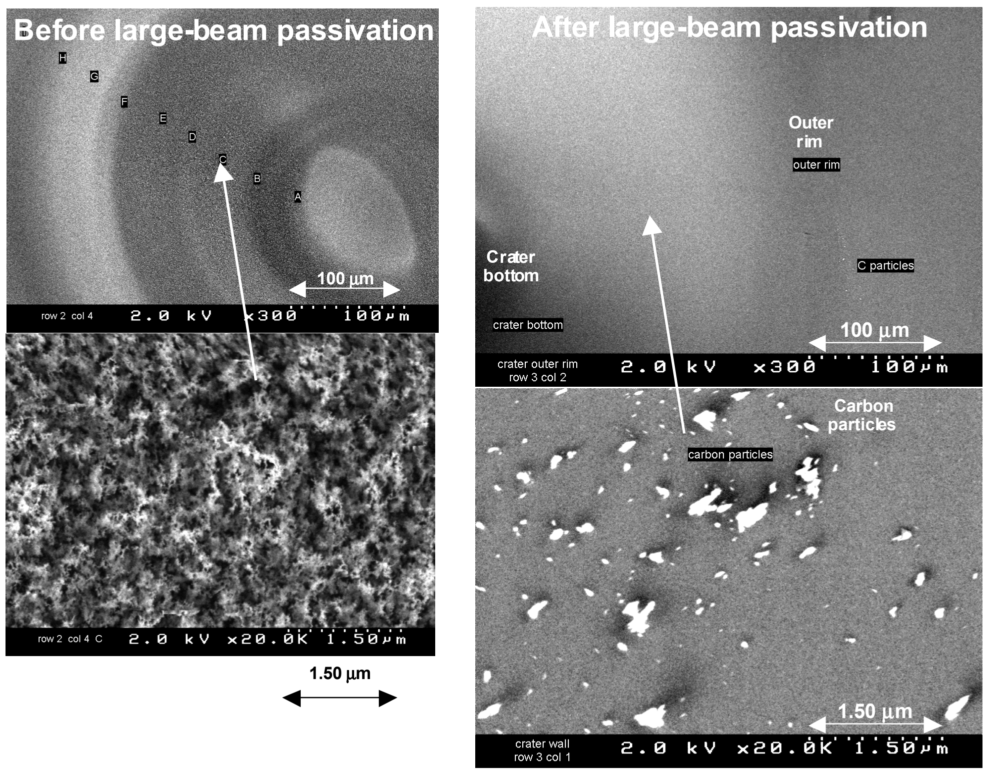

Fig. 4 High (20,000X) magnification SEM images of the walls of mitigation sites show that debris present as a fibrous structure prior to large beam passivation is converted to a specularly-smooth surface by the large beam passivation. The carbon particles were intentionally placed on the surface to facilitate focusing.

4. EFFECTS OF LARGE-BEAM PASSIVATION ON DAMAGE RESISTANCE

Damage tests were performed on sites mitigated using the new large-beam passivation. Both the testing method with the small, 355-nm, raster-scanned beam, and the one with multiple 10-ns shots of the 5-mm diameter, 351-nm beam were employed. Performance with the raster-scanned beam was equivalent to or superior to that achieved prior to large-beam passivation. Multiple-shot performance with the 5-mm diameter beam improved over previous results.

Tests with a raster-scanned beam were performed on 89 mitigation sites on undamaged fused silica (designated surrogate mitigation), and 20 sites of mitigated laser damage. The number of evaporation/passivation repetitions ranged from 1 to 27 for the surrogate mitigation sites, and from 3 to 9 repetitions for the mitigated damage sites. The depth of a mitigation site produced by 27 repetitions was ~200 μm (see Fig. 9 below for the dependence of depth on the number of repetitions). All 89 surrogate mitigation sites survived 7.5 ns, 355-nm pulses to 24 J/cm^2, and all 20 mitigated damage sites survived to 28 J/cm^2. This performance is as good as or superior to that achieved without large-beam passivation.

The results of the damage tests with the 5-mm diameter, 351-nm beam are summarized in Table 1. These were all performed on surrogate mitigation sites. Successful completion of this test involved ramping the fluence from 6 J/cm^2 to 12 J/cm^2 in ~100 shots, and then shooting 300 more shots at 12 J/cm^2 without damage. The test was terminated at the first indication of damage if damage occurred prior to completion. It is seen that there was a 100% success rate for

Number of Mitigation Repetitions	Number of Sites Tested	Estimated Depth of Sites from Fig. 9 (μm)	Number of Failures	Total Number of Shots at Failure or Test Completion	Fluence at Failure or Test Completion (J/cm^2, 351 nm)
2	3	50	0	>400	12
5	3	100	0	>400	12
9	3	120	0	>400	12
18	3	180	0	>400	12
27	3	205	2	1, 93	6, 12
36	3	220	3	1, 43, 73	6, 9, 10.7
45	3	230	3	1, 1, 1	6, 6, 6

Table 1 Results of damage tests of surrogate mitigation sites for multiple, 10-ns shots with a 5-mm diameter, 351-nm beam.

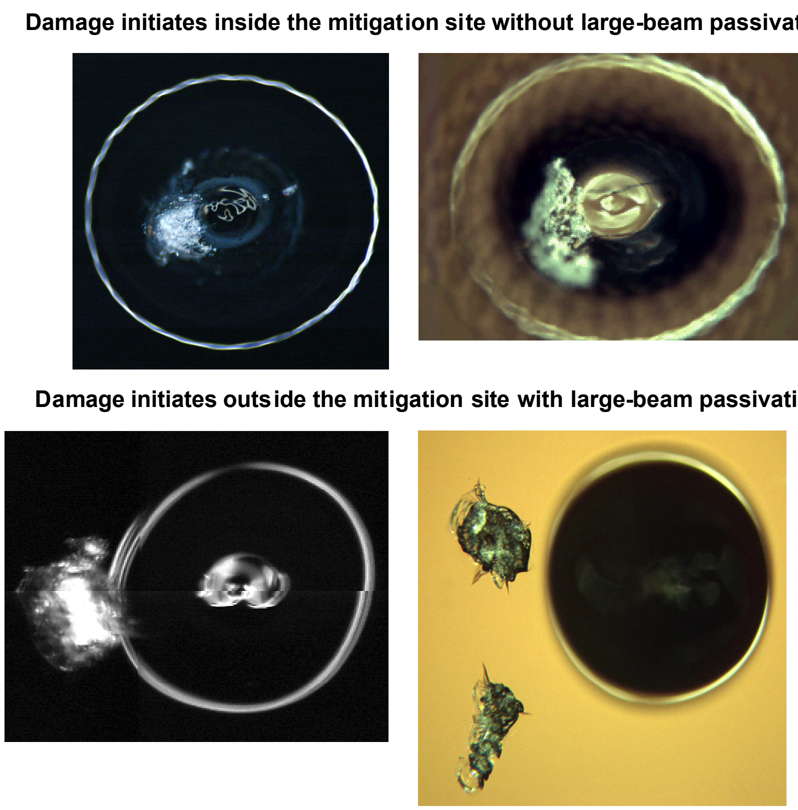

Fig. 5 Microscope images showing that damage initiated inside the mitigation sites without large-beam passivation, and initiated outside when large-beam passivation was applied. The images on the left are from tests with the small, raster-scanned, 355-nm beam. The images on the right are from tests with the 5-mm diameter, top-hat, 351-nm beam. The "dimpling" of the surface in the sites without large-beam passivation is caused by pulsed operation of the CO_2 laser at 5 kHz. The CO_2 laser was operated CW throughout the mitigation process when large-beam passivation was used.

mitigation sites with depths ~180 µm and less. This contrasts with the results without large-beam passivation where failure occurred for even the shallowest of mitigation sites.

We attribute this improvement to the elimination of debris by the large beam passivation. Without large-beam passivation this debris was always present, even in the shallowest mitigation sites. It then served as an initiator of damage in the multiple shot tests. This conclusion is further supported by the observation that the damage no longer initiated inside the mitigation site where debris was located prior to its elimination by large-beam passivation. It now always occurred outside the mitigation site for both methods of testing as seen in Fig. 5.

A new mechanism has come into play that causes the damage to initiate outside the mitigation in the absence of debris. One possible cause that we are now investigating is interference between the incident beam and light reflected specularly from walls of the mitigation site when it is located on the output surface of the optic (this is the case for all the damage tests reported here). Intensification from this interference would occur outside the mitigation site.

Also note in the images that a "dimpling" of the surface is absent with large-beam passivation. The dimpling was caused by the 5kHz pulsed operation of the CO_2 laser in the mitigation process without large-beam passivation. The laser was switched to CW operation at the same time that the process was modified to include large-beam passivation.

5. LARGE-BEAM PASSIVATION EFFECTS ON DOWNSTREAM INTENSIFICATION

Prior to the introduction of large-beam passivation, it was observed that the mitigation sites produced a strong, on-axis intensification of a 1064-nm beam transmitted through it as shown in Fig. 6. This of course is of concern because of the potential to damage NIF optics downstream of the mitigation site. Stylus profilometer measurements of mitigation site shapes showed a rise, or "mound" at the bottom (see Fig. 6). It is believed that this mound acts as a positive lens to produce the on-axis intensification (this hypothesis is under continuing investigation).

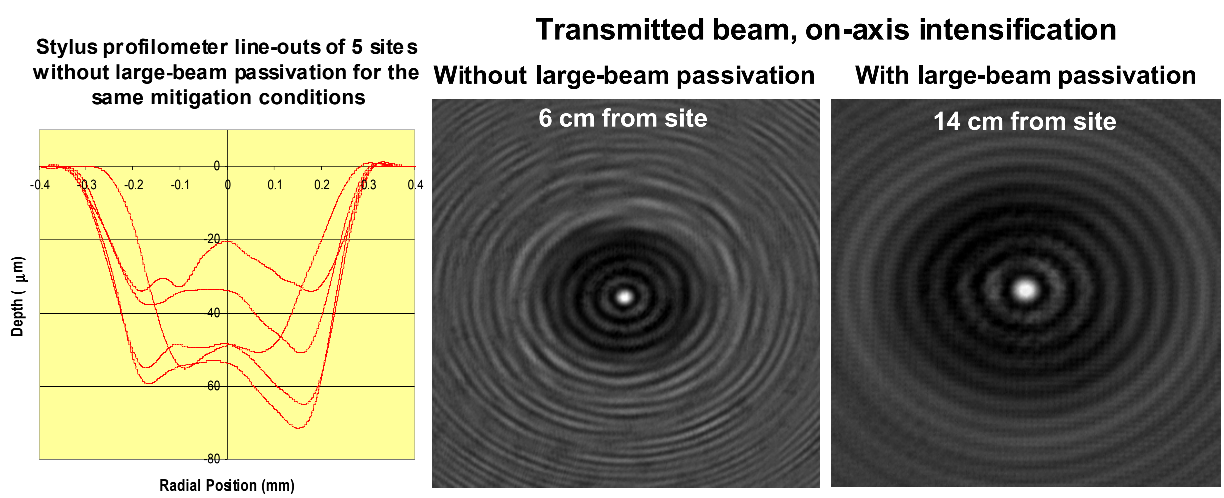

Fig. 6 The two images on the right show downstream, on-axis intensification of a 1064-nm laser beam transmitted through mitigations sites. The stylus profilometer line-outs on the left show a "mound" whose lensing is believed to produce the intensification. Large-beam passivation as now implemented is apparently insufficient to completely remove the mouind.

It was hoped that the smoothing effects of large-beam passivation would remove the mound and eliminate the intensification. Although this was apparently the case for the example shown in Fig. 3, it is obviously not always the case as evidenced by the intensification seen in Fig. 6. Preliminary observations are that large-beam passivation seems to be somewhat effective in eliminating or reducing the mound for shallower mitigation sites but become increasingly less effective for deeper sites. This is still being investigated. We expect to eliminate the mound by increasing the amount of evaporation at the bottom of the site during the evaporation spiral, and by increasing the large-beam passivation dwell time at the bottom.

6. PROCESS CONTROL AND REPEATABILITY

Process control is critical in the mitigation of high-value NIF optics, especially during the passivation phase near the evaporation threshold where small changes in laser power can cause large changes in the evaporation rate, and hence the generation of debris. A good metric of process control is repeatability of the process for the same conditions. Periodic fluctuations in the output power and spatial mode of our commercial, waveguide CO_2 laser prevented good repeatability (Fig. 7). These fluctuations have been observed in two such commercial CO_2 lasers. An AOM was inserted in the beam path to correct this problem by allowing active control of the power delivered to the sample (see Fig. 2).

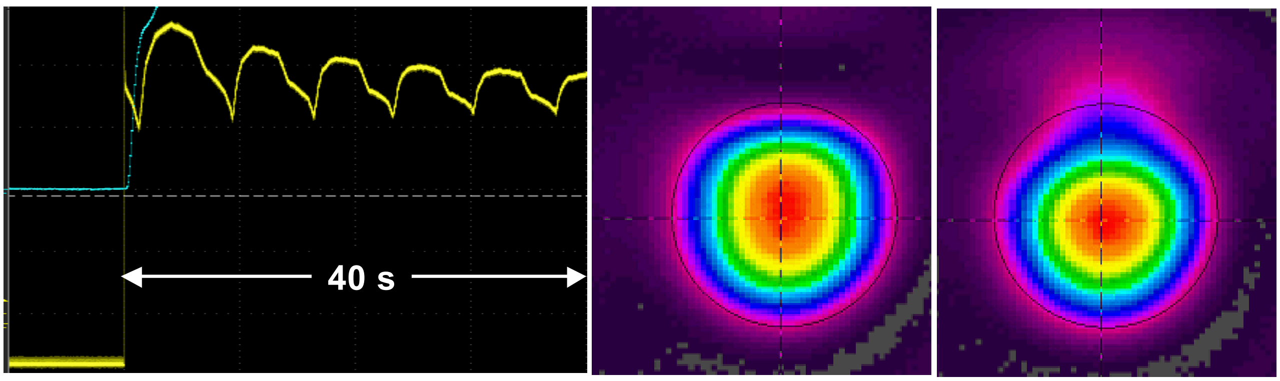

Fig. 7 The oscilloscope trace on the left shows period fluctuations in the output power of a commercial, waveguide CO_2 laser that affects the repeatability of the mitigation process. The spatial mode at the output of the laser also varies periodically between the two shapes on the right synchronously with the power fluctuations.

Control was not entirely successful as seen by the oscilloscope traces of Fig. 8 of the output of the AOM as measured by the photodiode used in the control loop (see Fig. 2), and of the power delivered to the sample as measured by a power meter. It is also evident in the graph of Fig. 9 where the variability of the depths of mitigation sites for a fixed number of evaporation/passivation repetitions did not change significantly after the control system was implemented.

We believe heating of the photodiode by the laser light, and spatial mode fluctuations on its sensor prevent the control loop from operating properly. We plan to address these problems by using a different type of CO_2 laser that does not have the power and spatial mode fluctuations (probably a DC discharge type), and a thermally insensitive photodiode (probably cryogenically cooled).

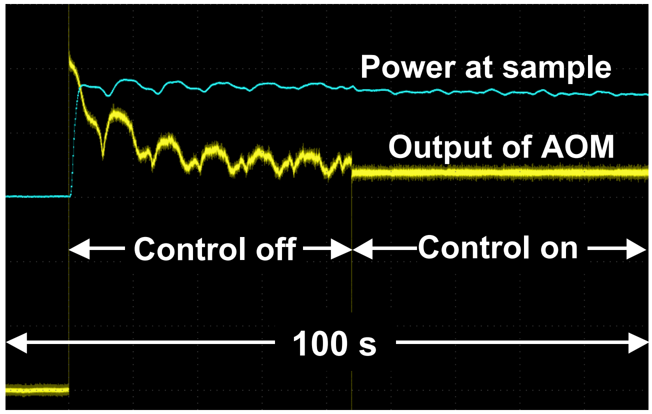

Fig. 8 Oscilloscope traces showing that active control of the laser power by an AOM did not eliminate fluctuations of laser power delivered to the sample. The initial drop in the output of the AOM with the control off is attributed to heating of the control photodiode (see Fig. 2), and the fluctuations of the power to the sample with the control on is attributed to spatial mode variations on the photodiode.

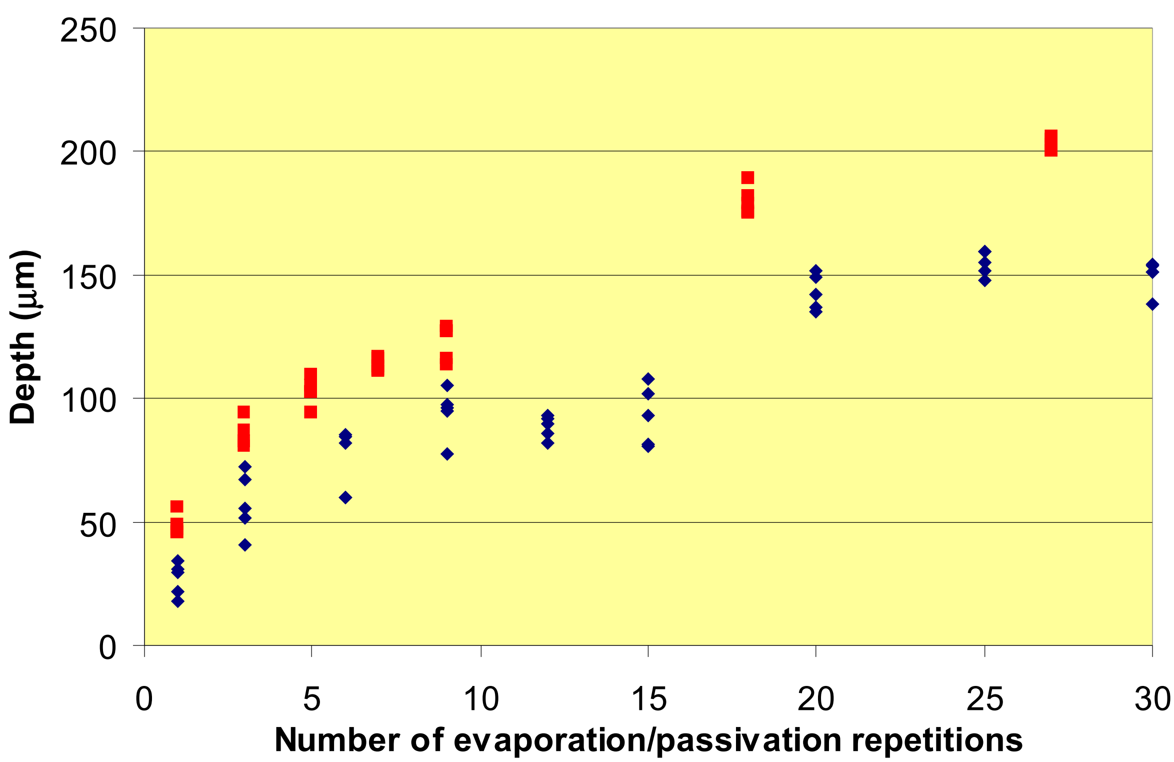

Fig. 9 Plots of the depth of mitigation sites versus the number of evaporation/passivation repetitions show comparable lack of repeatability for the same number of repetitions both before (diamonds) and after (squares) implementation of the active AOM control system.

7. SUMMARY

A previously reported and demonstrated technique[3] for mitigating the growth of large surface damage sites at 351 nm in high-value NIF optics at LLNL revealed several problems upon further investigation. The technique was based on fast galvanometer scanning of a tightly focused, 10.6-μm CO_2 laser spot over the area of the damage site. The most serious problem was re-initiation of laser damage to the mitigated sites at relatively low UV fluences. It was caused by debris re-deposited on the surface during the mitigation process. A new, final step was added to the mitigation process that re-melted, or passivated the debris with an enlarged, slowly scanned CO_2 laser spot that maintained the surface temperature just below the evaporation threshold. SEM studies showed that this completely converted the debris to a surface essentially the same as that of the original fused silica surface, and laser damage was no longer initiated by the debris. However, a new damage mechanism appeared which might be related to interference between the incident UV beam and reflections from the smooth walls of the mitigation site.

The large-beam passivation did not however correct the problem of downstream intensification caused by a mound that tends to form at the bottom of the mitigation site and appears to act as a focusing lens. We plan to correct this problem by increasing the amount of evaporation and the large-beam passivation dwell time at the bottom.

Yet another problem was poor process repeatability caused by fluctuations in the output power of the commercial, waveguide CO_2 laser. An AOM was inserted in the beam path to permit active control of the laser power. This did not completely correct the repeatability problem because of fluctuations in the spatial mode of the laser and heating of the photodiode used in the control loop. Plans to improve repeatability include the use of a more stable CO_2 laser and a thermally insensitive photodiode in the control loop.

8. ACKNOWLEDGMENTS

The authors gratefully acknowledge the contributions of Wren Carr (microscopy of NIF optics), Jim Ferreira (SEM), Bill Hollingsworth and Gene Donohue (large beam Nd:YLF/Glass damage testing), Laurie Lane and Rahul Prasad (excimer damage testing), Larry Platz (intensification measurements), Pam Whitman (mitigation of NIF optics), and Clay Widmayer (propagation calculations).

This work was performed under the auspices of the U. S. Department of Energy by the University of California Lawrence Livermore National Laboratory under contract No. W-7405-Eng-8.

9. REFERENCES

1. L.W.Hrubesh, M.A.Norton, W.A.Molander, E.E.Donohue, S.M.Maricle, B.M.Penetrante, R.M.Brusasco, W.Grundler, J.A.Butler, J.W.Carr, R.M.Hill, L.J.Summers, M.D.Feit, A.Rubenchik, M.H.Key, P.J.Wegner, A.K.Burnham, L.A. Hackel and M.R.Kozlowski, "Methods for mitigating surface damage growth on NIF final optics" in *Laser-InducedDamage in Optical Materials: 2001*, Proc. SPIE 4679, (2002).
2. R. M. Brusasco, B. M. Penetrante, J. A. Butler and L. W. Hrubesh, "Localized CO2 laser treatment for mitigation of 351 nm damage growth on fused silica" in *Laser-InducedDamage in Optical Materials: 2001*, Proc. SPIE 4679, 40-47 (2002).
3. I. L. Bass, G. M. Guss, R. P. Hackel, "Mitigation of Laser Damage Growth in Fused Silica with a Galvanometer Scanned CO2 Beam" in *Laser-InducedDamage in Optical Materials: 2005*, edited by Gregory J. Exarhos, Arthur H. Guenther, Keith L. Lewis, Detlev Ristau, M. J. Soileau, Christopher J. Stolz, Proc. SPIE Vol. 5991, 59910C (2005)